Impurity conduction at low compensation levels in Zn-doped InP

M. Benzaquen and B. Belache
McGill University, Rutherford Physics Building, 3600 University Street, Montreal, Quebec, Canada H3A 2T8

C. Blaauw
Bell-Northern Research, Ltd., P.O. Box 3511, Station C, Ottawa, Canada K1Y 4H7

(Received 9 February 1990)

We report on the impurity-conduction measurements, in the strong-localization regime, for *p*-type Zn-doped InP epilayers with low compensation levels. Both Hall-transport and magnetoresistance measurements were carried out. Variable-range hopping was present in all samples below 5 K, where Mott's full expression for the conductivity was found to give an excellent description of the data, with consistency between the theoretical predictions for the activation energies and the corresponding experimental values. Above 5 K, nearest-neighbor hopping was observed in all samples and was found to be consistent with a model by Efros and Shklovskii, provided that the effects of an enhancement of the dielectric constant at high doping levels were included. An unusual saturation of the low-temperature conductivity was observed in the purest epilayers. For layers with a low level of compensation, such an effect has been predicted by Shklovskii and Yanchev. However, their theory could only provide a qualitative explanation of our results.

I. INTRODUCTION

From a recent review by Mansfield,[1] it is clear that a considerable amount of data is presently available on the subject of hopping transport in *n*-type III-V compound semiconductors. The following trends have been extracted from those data for two regimes of the conduction.

A. Variable-range hopping conduction

In lightly doped material, at sufficiently low temperature (T), electrical transport is by means of variable-range hopping. The conductivity is generally of the form

$$\sigma=\Gamma_0 T^{-1/2}\exp[-(T_0/T)^s] \quad \text{with} \quad s=\tfrac{1}{4}\ , \tag{1}$$

where

$$T_0=49/(k_B D_0 a^3) \tag{2}$$

and

$$a=h/\sqrt{2m^* E_A}\ . \tag{3}$$

k_B is the Boltzmann constant, $\hbar$ is the Planck constant divided by 2π, m^* is the effective mass of the light holes ($m^*=0.08m_0$ in InP), and E_A is the binding energy.

Equation (1) was derived by Mott[2] by assuming a constant density of states D_0 in the impurity band at the position of the Fermi level (E_F).

In more heavily doped material, conductivity has sometimes been observed of the form

$$\sigma=\Gamma_0' T^{-1}\exp[-(T_0'/T)^s] \quad \text{with } s=\tfrac{1}{2}\ , \tag{4}$$

where

$$T_0'=10/(k_B C_0^{1/3} a)\ . \tag{5}$$

Equation (4) was derived by Efros and Shklovskii[3] by taking long-range Coulomb interactions into account, which, if not screened, lead to the presence of a Coulomb gap in the density of impurity states.

It is general practice to neglect the variation of the preexponential factors of Eqs. (1) or (4) in the analysis of the experimental data. In the temperature region where $T \ll T_0$, Mansfield[1] has shown that, although it does not affect the power in the exponential, this is in most cases inadequate and leads to the too small experimental values of T_0 generally observed. The use of Eqs. (1) or (4) for the conductivity is then required to provide adequate agreement with theory. In addition, when T is close to or larger than T_0, the preexponential factors of Eqs. (1) and (4) dominate their temperature dependence. The exponent s cannot then be accurately determined, even if the prefactor is taken into account.

B. Nearest-neighbor hopping conduction

At higher temperatures, a range is generally found where conduction is by nearest-neighbor hopping, with a conductivity of the form[4]

$$\sigma=\Gamma_3 T^{-1}\exp(-T_3/T)\ , \tag{6}$$

where

$$\Gamma_3=\beta_3 T_3 a^{-3}(N_A^{1/3}a)^{-0.15}\exp[-\alpha/(N_A^{1/3}a)] \tag{7}$$

and

$$T_3=0.61T_D\ . \tag{8}$$

T_D is the temperature corresponding to the energy of the Coulomb interaction at the average distance between majority impurities and is given by

 ©1990 The American Physical Society

$$T_D=(4\pi/3)^{1/3}q^2N_A^{1/3}/(k_Bk)\ . \tag{9}$$

N_A is the majority dopant concentration, β_3 a constant, q the electronic charge, k the low-frequency dielectric constant ($k=12.35$ for InP), and $\alpha=1.73$. This value of α is well established[4] for impurities with isotropic wave functions.

In Eq. (6), the preexponential temperature variation is generally neglected, in the determination of T_3, which is only justified[1] if $T\ll T_3$. Under those conditions, the available experimental data is in good agreement with theory if the variation of the dielectric constant with carrier concentration is taken into account.[1]

Equation (6) then becomes

$$\sigma=\sigma_3\exp(-T_3'/T)\ . \tag{10}$$

In the above models, the contribution of the heavy holes to the conduction is not taken into account due to the small overlap of their wave functions.

C. Hopping conduction in *p*-type material

Detailed experimental data on the hopping conduction of *p*-type semiconductors is still relatively rare. The early work of Fritzsche and Lark-Horowitz[5,6] on *p*-type Ge provided evidence for nearest-neighbor hopping. Also in *p*-type Ge, Shlimak and Nikulin[7] found Eq. (1) in agreement with their purest sample, while a more heavily doped sample showed a behavior consistent with Eq. (4). More recently, Kuznetsov *et al.*[8] studied the impurity conduction of InP:Mn for samples falling well below the corresponding Mott transition. They found Eq. (10) in excellent agreement with their experimental data, with values of T_3 very close to those theoretically predicted. In addition, at lower temperature, Mott's law was verified from 4 to 39 K, with $T\ll T_0$ and a variation of the conductivity of seven decades, leaving little doubt about the accuracy of their result. The value of T_0 extracted was in excellent agreement with Mott's theory.

In this article, we present the results of impurity-conduction measurements on a series of *p*-type Zn-doped InP epilayers, grown by metalorganic chemical vapor-deposition (MOCVD) on semi-insulating Fe-doped InP substrates. Both Hall transport and magnetoresistance measurements were carried out. In previous articles, we presented experimental details pertaining to the MOCVD system,[9] characterization of the dopant profiles by secondary-ion mass spectroscopy (SIMS),[10] preparation of samples for electrical transport measurements[11] and the execution of those measurements.[11]

II. RESULTS AND DISCUSSION

A. Extended-states Hall data

In this section we summarize extended-states Hall results reported earlier[10] for samples 1, 2, and 4. Relevant data, including nomenclature of the samples as used in Ref. 10, are presented in Table I. [Zn] is the Zn concentration as determined by secondary-ion mass spectroscopy, N_A and N_D are the acceptor and donor concentration, respectively, p_R is the total hole concentration at room temperature, K the compensation ratio defined as N_D/N_A, and a is given by Eq. (3). E_A was extracted from freeze-out statistics between 35 and 100 K for samples 1 and 2, and between 70 and 140 K for samples 3 and 4. E_A decreased with increasing doping level, as expected when the Mott transition is approached. Strong excitation to the valence band was still evident, at room temperature, in the more heavily doped samples.

The temperature variation of the total hole concentration p is given by the expression[12]

$$p=\tfrac{1}{2}\{-(N_D+N_v)+[(N_D+N_v)^2+4N_v(N_A-N_D)]^{1/2}\}\ , \tag{11}$$

where

$$N_v=2(2\pi m^*k_BT/h^2)^{3/2}\beta\exp(-E_A/k_BT)\ .$$

β is the degeneracy factor of the acceptor level, k_B the Boltzmann constant, h the Planck constant, and m^* the density of states effective mass. Equation (11) was fitted to our experimental data with the appropriate values of E_A, β, and m^* with N_A and N_D as adjustable parameters.[10] A good simultaneous fit of the hole concentration and the mobility was obtained for samples 1, 2, and 4, of which the results are quoted in Table I. The values of N_A were in excellent agreement with the SIMS data[10] (Table I). The value of N_A quoted for sample 3, which is the most heavily doped of the set, is about a factor 2 larger than [Zn]. This discrepancy is attributed to a decrease of the Hall factor–which was found close to 1 for the other samples[10]—at higher doping levels.

B. Conductivity at low doping levels

Figure 1 shows a linear plot of the conductivity σ of samples 1 and 2 in the temperature range of 3 to 30 K. For the sake of clarify, only a fraction of the available experimental points is shown. Below approximately $T=11$ K, σ exhibits an activated behavior which saturates at

TABLE I. Parameters extracted from the high-temperature data for all samples.

Sample no.	[Zn] (cm^{-3})	N_A (cm^{-3})	N_D (cm^{-3})	E_A (meV)	P_R (cm^{-3})	K	a (Å)
1 ("*B*313")	1.5×10^{17}	1.42×10^{17}	1.51×10^{16}	41.0	1.13×10^{17}	0.106	34.08
2 ("*B*316")	7.0×10^{16}	6.94×10^{16}	1.12×10^{16}	42.7	5.45×10^{16}	0.161	33.40
3 ("*B*274")	1.2×10^{18}	2.74×10^{18}	2.10×10^{17}	25.9	1.23×10^{18}	0.076	42.88
4 ("*B*276")	9.0×10^{17}	1.15×10^{18}	1.20×10^{17}	26.2	7.46×10^{17}	0.104	42.63

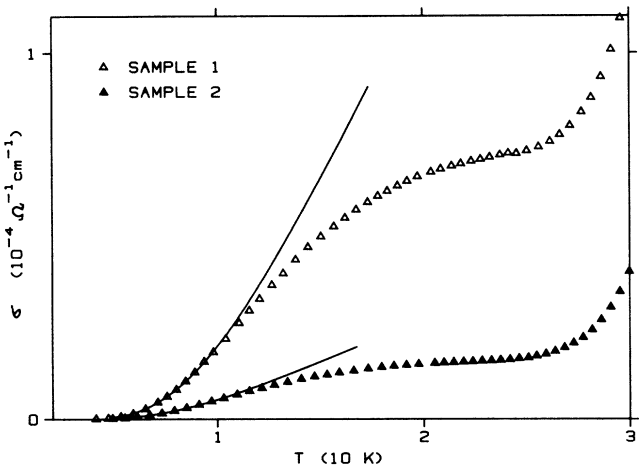

FIG. 1. Conductivity as a function of temperature for samples 1 and 2. The continuous lines correspond to nearest-neighbor hopping as given by Eq. (10) with the parameters quoted in Table II.

higher temperatures. Above 26 K, the beginning of a large increase of σ with temperature is shown, which extends over many decades at higher temperature.

Figure 2 shows the variation of the Hall coefficient R_H of sample 1 with temperature in the range of 4–50 K. The sign of R_H remains the same in the whole temperature range. A peak is observed in R_H at a temperature $T_P \approx 31$ K. A similar result was first observed by Hung in Ge[13] and is due to conduction by two decoupled bands.[14,15] The peak occurs at the temperature where the contribution of each of the bands to the conduction is of equal importance. In our case, for $T > T_P$, the valence band dominates the conduction. As the free hole concentration rises exponentially, with a simultaneous increase of the corresponding mobility, the conductivity undergoes an extremely fast increase. This corresponds to the behavior partly shown in Fig. 1 above 26 K. Using a two-band model, it can be shown that the importance of one band relative to the other, for the conduction, decreases rapidly as T moves away from T_P and becomes negligible[16] at the basis of the peak of R_H. Consequently, in the case of Fig. 2, the onset of pure extended states conduction is at about 45 K, and pure hopping conduction occurs below 26 K. The relatively flat behavior of R_H observed between 11 and 26 K is very unusual and corresponds to the saturation of the activated behavior shown in Fig. 1. It could indicate an approximately constant mobile carrier concentration. Below 11 K, R_H undergoes an extremely large increase, which extends over several orders of magnitude as T is decreased (not fully shown). This behavior has previously been observed in the strong localization regime of n-type InP,[14,17] and is consistent with a decrease of the concentration of hopping carriers with decrease temperature. However, in the case of n-type InP, no flat region was observed between the two-band peak and the increase of R_H at low temperature.

Figure 3 shows the Hall mobility μ_H of sample 1 between approximately 11 and 26 K. A relatively flat region is observed from 15 to 23 K, roughly corresponding to the flat region of both σ and R_H. Below 11 K, μ_H could not be accurately measured due to the high noise level.

Figure 4 shows the low-field transverse magnetoresistance of sample 1 as a function of temperature. The magnetic induction was 4 kG. Two temperature regions of distinct behavior are again observed. For $T < 11$ K, corresponding to the activated region of Fig. 1, the negative magnetoresistance is relatively large and increases with decreasing temperature. A similar trend has been observed[18] in the strong localization regime of n-type GaAs and found in fair agreement with a model proposed by Fukuyama and Yosida.[19] According to this model, the

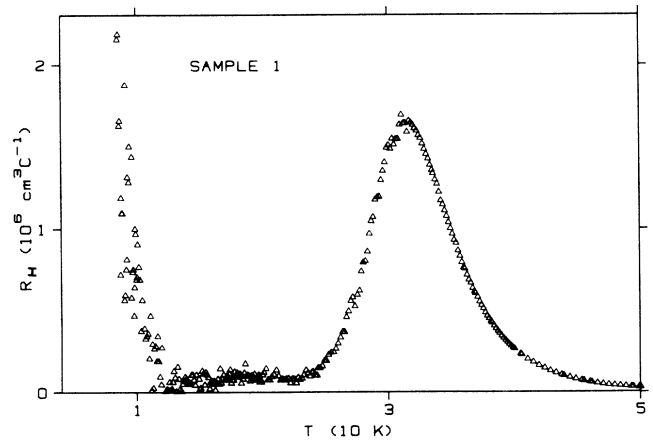

FIG. 2. R_H as a function of temperature for sample 1. The flat region between 11 and 25 K corresponds to the saturation of the nearest-neighbor-hopping regime. The increase of R_H below 11 K is linked to hopping conduction. The peak at $T_P \approx 31$ K is due to two-band conduction.

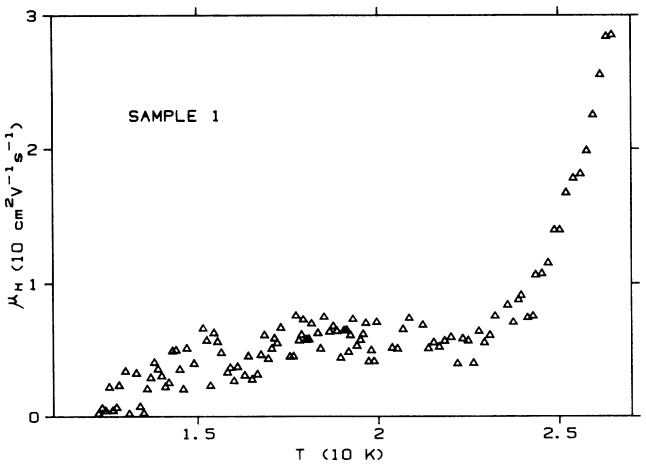

FIG. 3. Hall mobility of sample 1 as a function of temperature.

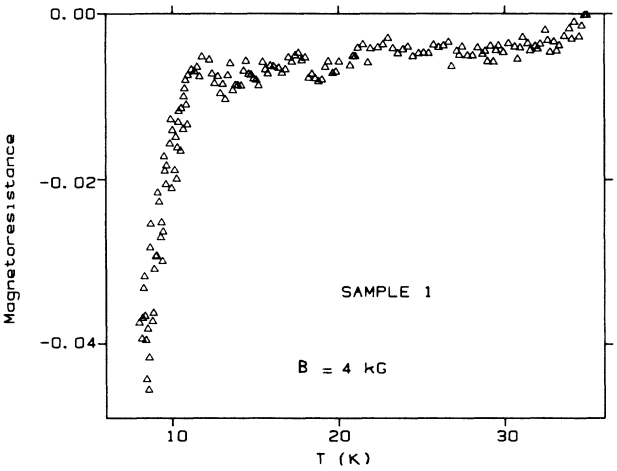

FIG. 4. Transverse magnetoresistance of sample 1 as a function of temperature at $B=4$ kG. A significant decrease of the magnetoresistance is observed below 11 K, corresponding to the hopping regime. The flat behavior from 11 to 30 K corresponds to its saturation. The magnetoresistance becomes positive above $T=33$ K, where the valence bands dominate electrical transport.

magnetic field causes a Zeeman splitting of the impurity states, with a majority of carriers in the upper state, which offers a better overlap of the electronic wave functions and leads to a significant increase of the conductivity. In the temperature region of 11–30 K, the negative magnetoresistance is considerably smaller and relatively flat. This region corresponds to the saturation region of Fig. 1. However, we point out that the uniformity of our samples is estimated to be of the order of 2%. Because of the presence of the Hall voltage, the contacts used for the measurement of the magnetoresistance have to be considered independent, for the purpose of the error calculation of the experimental magnetoresistance. Consequently, the error bar, in Fig. 4, is of the order of 2%, i.e., four times as large as the value of the magnetoresistance in this region. Therefore, the data above 10 K are only indicative of a possible behavior. Above approximately 31 K (corresonding to T_P in Fig. 2), the magnetoresistance becomes positive, as expected when extended-states conduction is dominant.

Shklovskii and Yanchev[20] considered the possibility of saturation of the nearest-neighbor hopping regime in the case of low compensation. At sufficiently low temperature, this corresponds to a nearly full impurity band. For p-type material, the majority of localized impurity states are occupied by holes, with the compensating impurities binding N_D electrons. As the temperature increases, the electrons start to thermally break away from their location and become available for the hopping process. This mechanism reaches saturation when the concentration of the electrons allowed to hop reaches N_D. Further growth of the break-away electrons then becomes impossible. Such an effect should exist for all levels of compensation at sufficiently high temperature. Nevertheless, its direct observation is likely to be hidden by the onset of extended-states conduction. In fact, when activated conduction is observed at low temperature and electrical transport in the conduction band is precisely modeled, the low-temperature peak of R_H, which is usually observed, cannot generally be reproduced by extrapolation to higher temperature of the observed electrical behavior of the impurity carriers.[21] Even when not directly observed, saturation of the activated behavior should take place in a temperature range where extended-states conduction is dominant. The temperature T_s at which this effect occurs depends both on compensation and on the width of the band. Shklovskii and Yanchev[4] give the following estimate:

$$T_s = T_3' / \ln(N_A/N_D) \ . \tag{12}$$

Their quantitative model is based on the calculation of the position of E_F at finite temperature and leads to the following equation:

$$N_D \exp(-X^3) = 7.14\times 10^{-4} X^6 N_D + N_A \exp[-T_D/(TX)] \ , \tag{13}$$

where

$$X = k_B T_D / E_F \ . \tag{14}$$

The determination of X in Eq. (14) leads to the following expression for the conductivity:

$$\sigma = \sigma_3 \exp[-T_D/(TX)] \tag{15}$$

which, at sufficiently low temperature is equivalent to Eq. (10) with T_D given by Eq. (8).[4]

This model does not take into account the temperature dependence of the prefactor of the nearest-neighbor hopping conductivity. Consequently, for comparison purposes, we plot in Figs. 5 and 6 $\ln(\sigma)$ as a function of $1/T$, for samples 1 and 2, respectively, between approximately

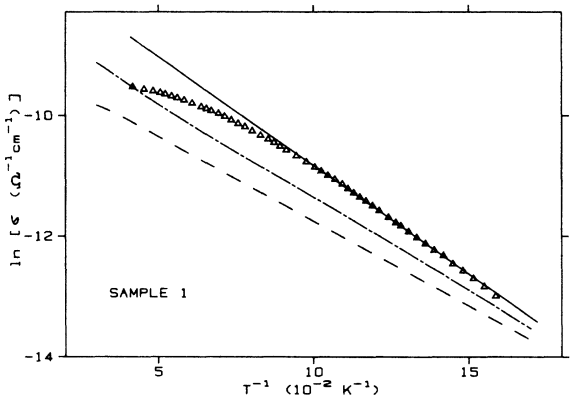

FIG. 5. $\ln(\sigma)$ as function of $1/T$ for sample 1. The continuous line is the fit of Eq. (10) to the data. The dashed line was obtained from Eq. (13) and the parameters quoted in Tables I and II. The dashed-dotted line shows the effect of an increase in compensation. All three lines merge at $T<2$ K.

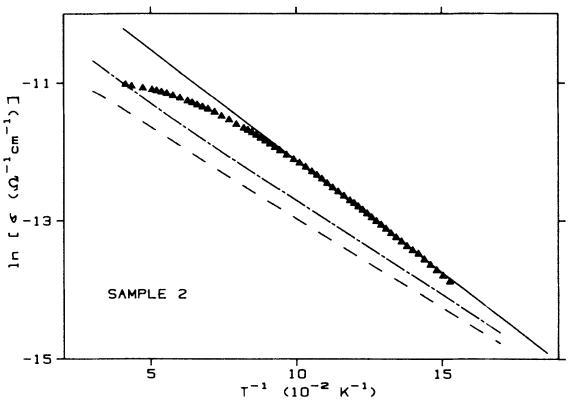

FIG. 6. $\ln(\sigma)$ as function of $1/T$ for sample 2. The continuous line is the fit of Eq. (10) to the data. The dashed line was obtained from Eq. (13) and the parameters quoted in Tables I and II. The dashed-dotted line corresponds to an increase in compensation. All three lines merge at $T<2$ K.

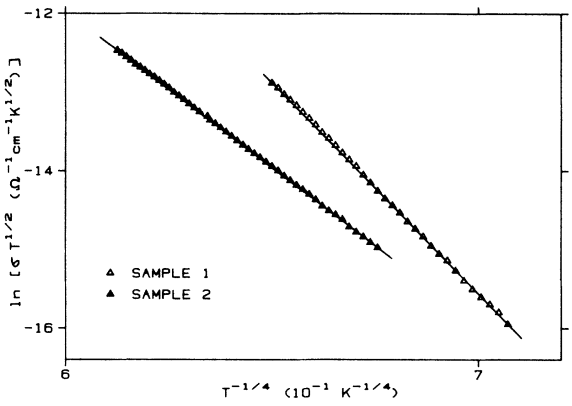

FIG. 7. $\ln(\sigma T^{1/2})$ as a function of $T^{-1/4}$ for samples 1 and 2. Mott's law is well verified at sufficiently low temperature. The continuous lines are the fits of Eq. (1) to the data.

6 and 26 K. The continuous lines are the fits of Eq. (10) to the data in the range of approximately 6 to 11 K. The values of σ_3 and T_3' obtained experimentally are quoted in Table II along with T_s [Eq. (12)] and the theoretical values of T_3 [Eq. (9)]. For both samples, T_s falls in the observed saturation region and is reasonably close to its onset (11–12 K). However, the theoretical values of T_3 are almost a factor 2 larger than the experimental ones. Two reasons can explain this discrepancy. On the one hand, the experimental values of T_3' are not very much larger than the temperatures of the range under consideration. The prefactor of Eq. (6) should then be considered and would increase the experimental T_3. On the other hand, Eq. (9) shows that T_3' is inversely proportional to the dielectric constant, for which an enhancement is likely at the doping levels of our samples. This should decrease the theoretical value of T_3'. As expected for nearest-neighbor hopping, the activation energy decreases with decreasing doping level. With the values of σ_3 quoted above, T_D follows immediately from Eq. (8) and is also quoted in Table II. With N_A and N_D given in Table I, Eq. (13) can be solved numerically for X as a function of temperature. The theoretical conductivity is then obtained with Eq. (15). It is shown as a dashed line in Figs. 5 and 6. The dashed-dotted lines were obtained with $N_D=5\times10^{16}$ cm^{-3} for sample 1 and $N_D=2.5\times10^{16}$ cm^{-3} for sample 2, with all other parameters remaining unchanged. This gives an indication of the sensitivity of the model, for fixed T_D, with respect to compensation.

At temperatures lower than those shown in Figs. 5 and 6 (between 1 and 2 K), the lines generated with the above model merge with the continuous line, which corresponds to unsaturated nearest-neighbor hopping. Although theory qualitatively describes the deviation from the continuous line which is experimentally observed, a significant discrepancy remains. The onset of saturation occurs at a temperature much higher ($T\approx11$ K) than predicted by the model ($T\approx2$ K), and the observed deviation from the unsaturated region is more abrupt (Figs. 5 and 6). The variation of both R_H (Fig. 2) and the magnetoresistance (Fig. 4) with temperature at the onset of saturation (11–12 K) is also abrupt. Part of the discrepancy may be due to the fact that the temperature dependence of the prefactor of the nearest-neighbor hopping conductivity was neglected in the derivation of the model presented above. Nevertheless, we point out that from approximately 11 to 25 K, all the experimental quantities shown in Figs. 1 to 6 exhibit the behavior expected for a metal, while strong localization is evident below 11 K. This could be consistent with a temperature-induced metal-insulator transition of the Mott kind. Because of screening by the mobile carriers, the overlap of their wave functions is expected to increase with increasing temperature. In addition, for samples with low compensation as in the present work, the disorder in the impurity distribution should also be low. An indication of this is that the experimental values of T_3' are found to be lower than the theoretical predictions. A combination of those two effects could lead to the formation of a percolation path at a given temperature.

TABLE II. Parameters of samples 1 and 2 corresponding to Eqs. (8), (9), (10), and (12).

Sample no.	σ_3 (Ω^{-1} cm^{-1})	T_3'(expt.) (K)	T_3'(theor.) (K)	T_s (K)	T_D (K)
1	7.15×10^{-4}	35.81	69.51	15.96	58.70
2	1.35×10^{-4}	32.25	54.75	17.71	52.87

TABLE III. Parameters corresponding to Mott's variable-range hopping for all samples.

Sample no.	Γ_0 (Ω^{-1} cm^{-1} K$^{1/2}$)	T_0(expt.) (K)	s	D_0 (ergs^{-1} cm^{-3})	T_0(theor.) (K)	T range (K)
2	1.03×10^{5}	1.98×10^{6}	0.253	3.73×10^{30}	2.55×10^{6}	4.7–7.3
1	5.69×10^{9}	9.97×10^{6}	0.248	7.17×10^{30}	1.25×10^{6}	3.9–5.7
4	4.37×10^{6}	6.69×10^{4}	0.345	4.28×10^{31}	1.07×10^{5}	3.1–4.8
3	4.97×10^{7}	6.32×10^{5}	0.283	9.72×10^{31}	4.63×10^{4}	4.8–6.8

At the lowest temperatures investigated, a clear deviation from the nearest-neighbor hopping regime is observed for samples 1 and 2, and the corresponding data for σ is shown in Fig. 7. Equation (1) was fitted to the data in the temperature range indicated in Table III, with Γ_0, T_0, and s as free parameters. The continuous lines of 3 were generated with the values of those parameters, quoted in Table III. Mott's law is in excellent agreement with the data. Although the temperature range where it is observed is limited due to the large resistance of the samples, the number of experimental points is high, and the corresponding variation of σ is of the order of two decades for both samples. The average relative error of both fits is below 5×10^{-3}. The results are therefore accurate.

C. Conductivity at higher doping levels

As shown in Table I, samples 3 and 4 are more heavily doped than the previous ones, but have similar low compensation. For both samples, the behavior of R_H for $T>22$ K is similar to that shown in Fig. 2 for sample 1, indicating two-band conduction. However, the two-band peak is much larger and extends up to 100 K. Such a feature is consistent, for those more heavily doped samples, with the larger impurity conduction expected.[14] No flat behavior is observed below 22 K, and R_H undergoes a fast increase with decreasing temperature in this region. This indicates that any saturation of hopping conduction will probably be hidden by extended-states conduction and not experimentally detected.

Figure 8 shows a plot of $\ln(\sigma T)$ as a function of $1/T$ for samples 3 and 4. The behavior is well described by Eq. (6), which corresponds to nearest-neighbor hopping. For sample 3, Eq. (6) was fitted to σ_3 between 7.5 and 21 K, and for sample 4 between 6 and 20 K. In both cases Γ_3 and T_3 were unconstrained. The resulting values of Γ_3 and T_3 are quoted in Table IV. Equation (6) was also fitted to σ for samples 1 and 2 in the appropriate temperature range. Those results are also reported in Table IV. By comparing the new values of T_3 with the ones obtained without the prefactor, we observe a significant increase, which brings them closer to the theoretically predicted values. The discrepancy for samples 3 and 4 is much larger, but this was expected for heavily doped samples, as discussed above, because of the enhancement of the dielectric constant which is not taken into account in the theoretical model.[1] Equation (10), when fitted to the data, gives a slightly lower relative average error than Eq. (6). Using T_3 instead of T_3' (Table IV, experimental value) in Eq. (12), with the values of N_A and N_D in Table I, we obtain $T_s=24.2$ K for sample 3 and $T_s=26.2$ for sample 4. This result further explains the fact that no saturation of the nearest-neighbor hopping regime is observed: the onset appears to occur in a temperature range where the effect of the valence bands is important or even dominant. In the temperature range indicated in Table III, samples 3 and 4 both show Mott's variable-

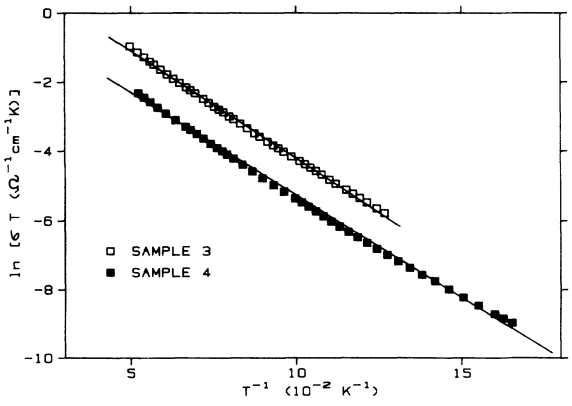

FIG. 8. $\ln(\sigma T)$ as a function of $1/T$ for samples 3 and 4. Nearest-neighbor hopping is observed with a variation of the conductivity of the order of 5 decades. The continuous lines are the fits of Eq. (6) to the data.

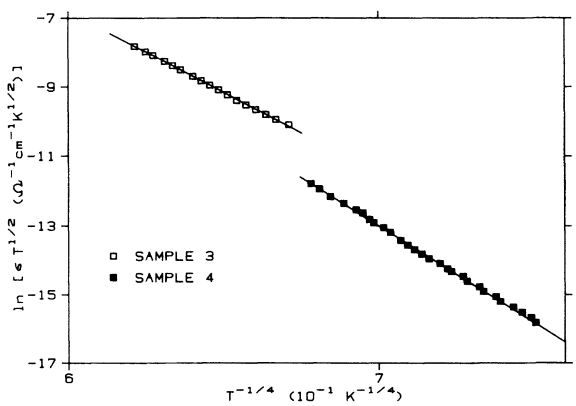

FIG. 9. $\ln(\sigma T^{1/2})$ as a function of $T^{-1/4}$ for samples 3 and 4 at very low temperature. Mott's law is observed in a narrow temperature range, with a variation of σ of 2 decades. The continuous lines are the fits of Eq. (1) to the data.

TABLE IV. Parameters corresponding to nearest-neighbor hopping for all samples.

Sample no.	Γ_3 (Ω^{-1} cm^{-1} K)	T_3(expt.) (K)	T_3(theor.) (K)	$1/(N_A^{1/3}a)$	T_D (K)	Y (Ω^{-1} cm^2)
2	3.271×10^{-3}	41.07	54.75	7.286	67.33	2.202×10^{-24}
1	1.519×10^{-2}	43.67	69.51	5.624	71.59	1.063×10^{-23}
4	1.958	59.32	139.59	2.239	97.25	2.268×10^{-21}
3	7.582	62.33	186.44	1.667	102.18	8.881×10^{-21}

range hopping. The data are shown in Fig. 9, with the corresponding fits of Eq. (1) to σ. The values of Γ_0, T_0, and s, obtained with an iterative least-squares-fit technique, are reported in Table III. Equation (3) gives the theoretical prediction for T_0. There, a is known and is quoted in Table I. A rough estimate of the density of states D_0 at E_F can be obtained as follows. T_D in Eq. (8) corresponds to the half-width of the impurity band.[4] If a constant density of states is assumed and if spin degeneracy is neglected, $D_0=N_A/(2k_BT_D)$ can be calculated and is reported in Table IV for all samples. The corresponding theoretical values of T_0 are given in Table III. Theory is in good agreement with experiment, as predicted by Mansfield,[1] when the prefactor of the variable-range hopping expression is taken into account. The largest discrepancy, observed for sample 3, corresponds to 1 order of magnitude. This is small compared to the much larger discrepancies previously reported[1] and can be attributed to the inconsistency, mentioned above, between the Hall analysis and the SIMS data of this sample. The value of N_A 50% lower suggested by SIMS gives much better agreement.

The theoretical value of $\alpha=1.73$, in Eq. (7), can be experimentally verified using the data extracted from the nearest-neighbor hopping regime of all samples. If we define

$$Y=\Gamma_3 a^3(N_A a)^{0.15}/T_3 , \tag{16}$$

a plot of $\ln(Y)$ as a function of $X=1/(N_A^{1/3}a)$ should, according to theory, yield a straight line with slope $-\alpha$. The values of X and Y obtained for each sample are quoted in Table IV. Figure 10 shows the corresponding plot. The continuous line is the best fit to the data and gives $\alpha=1.488$, in fair agreement with theory. A discrepancy is expected when some anisotropy of the carrier wave function is present,[4] which could be the case for our samples.

An interesting feature of the conductivity of samples 3 and 4 is shown in Fig. 11. For sample 3, Eq. (2), which corresponds to variable-range hopping conduction in the presence of a Coulomb gap in the impurity-band density of states, also provides a good description of the data between 5 and 16 K. The same is true for sample 4 between 3.2 and 12 K. There is no evidence for such an effect in samples 1 and 2. This shows that a combination of Eq. (1) at low temperatures and Eq. (6) at higher temperatures can give a relationship similar to that given by Eq. (2). It also shows that a temperature range can be found where Eq. (6) alone can yield values of the conductivity extremely close to those obtained with Eq. (2) and an appropriate choice of the respective parameters. The best fit of Eq. (2) to the data of sample 3, shown in Fig. 11, gave $\Gamma_0'=1.78\times10^3\ \Omega^{-1}\,\mathrm{cm}^{-1}\,\mathrm{K}$, $T_0'=1.29\times10^3$ K, and $s=0.507$. For sample 4, the corresponding results were $\Gamma_0'=1.36\times10^2\ \Omega^{-1}\,\mathrm{cm}^{-1}\,\mathrm{K}$, $T_0'=5.64\times10^2$ K, and $s=0.579$. In Eq. (5), C_0 is linked to the density of states near E_F by the expression[1]

$$g(E)=C_0E^2 ,$$

where $g(E)$ is the density of states and E the energy.

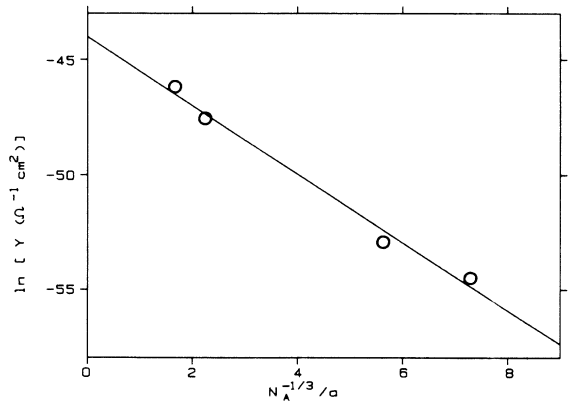

FIG. 10. $\ln(Y)$, as given by Eq. (16), as a function of $N_A^{1/3}/a$. The straight line, which represents the best fit to the data, has a slope $-\alpha=-1.488$.

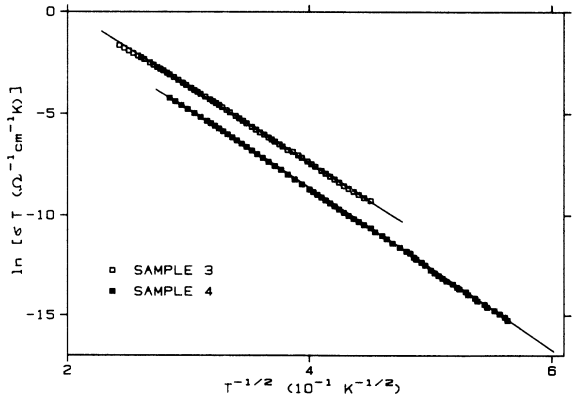

FIG. 11. $\ln(\sigma T)$ as function of $T^{-1/2}$ for samples 3 and 4. The continuous lines are the fits of Eq. (2) to the data.

This expression describes a Coulomb gap in the density of states. The determination of T_0 in Eq. (5) requires an estimate of C_0, which can be obtained as follows. The width of the impurity band is approximately $2k_BT_D$, with N_A energy states. If we assume that $g(E)$ is constant everywhere except at the Coulomb gap, for which we take a width of k_BT_D, it is easily verified that this leads approximately to

$$C_0=8N_A/(3k_B^3T_D^3)$$

by substituting this value in Eq. (5):

$$T_0'=7.21T_D/(N_A^{1/3}a) .$$

For sample 3, the last expression gives $T_0'=1.23\times10^3$ K, which is extremely close to the experimental value. This number would be increased by 25% if N_A had been determined from the SIMS data. For sample 4, we calculated $T_0'=1.57\times10^3$ K, which is an order of magnitude larger than the experimental result.

The analysis presented above shows the difficulty involved in distinguishing between Eqs. (1), (2), and even (6) for samples with a relatively high doping level. This difficulty is further increased by the fact that in such cases the parameters of all the corresponding theories are in fair agreement with experiment.

III. CONCLUSIONS

In conclusion, we have presented impurity conduction data for Zn-doped epitaxial layers of InP growth by MOCVD, with doping levels ranging from 7×10^{16} to 1.2×10^{18} cm^{-3}. All of the epilayers showed Mott's variable-range hopping at very low temperatures, with values of the activation energy which were in fair agreement with the corresponding model, in which the temperature dependence of the prefactor of the expression describing the conductivity was taken into account.

At higher temperatures, the results were consistent with nearest-neighbor hopping for all samples. Saturation of the conductivity with increasing temperature was observed in the case of the more lightly doped samples. A model by Shklovskii and Yanchev was found to be in qualitative agreement with the data, and could explain why saturation was not observed for more heavily doped samples. The activation energy of the nearest-neighbor hopping regime is consistent with theory if an enhancement of the dielectric constant at high doping levels is taken into account. The exponential dependence of the hopping conductivity on the acceptor concentration is also in good agreement with theory.

The conductivity of the more heavily doped samples could also be interpreted as a result of variable-range hopping in the presence of a Coulomb gap, followed, at higher temperatures, by nearest-neighbor hopping. This effect is consistent with several other observations in semiconductors close to the Mott transition.[1] However, an interpretation on the basis of a Coulomb gap is inconsistent with the fact that the vast majority of existing data for lightly doped samples unequivocally supports Mott's law[1,8] in crystalline semiconductors. Moreover, an unscreened Coulomb interaction would be expected either for lightly doped samples or at very low temperatures. No support for this is provided by our data.

[1] R. Mansfield, in *Hopping Transport in Solids,* edited by M. Pollak and B. I. Shklovskii (Elsevier, Amsterdam, 1988).

[2] N. F. Mott, Philos. Mag. **19**, 835 (1969).

[3] B. I. Shklovskii, Fiz. Tekh. Poluprovodn. **6**, 1197 (1972) [Sov. Phys.—Semicond. **6**, 1053 (1973)]; A. L. Efros and B. I. Shklovski, J. Phys. C **8**, L49 (1975).

[4] B. I. Shklovskii and A. L. Efros, in *Electronic Properties of Doped Semiconductors,* edited by M. Cardona, P. Fulde, and H.-J. Queisser (Springer-Verlag, Berlin, 1984), p. 190.

[5] H. Fritzsche, Phys. Rev. **99**, 406 (1955).

[6] H. Fritzsche and K. Lark-Horovitz, Phys. Rev. **113**, 999 (1959).

[7] I. S. Shlimak and E. I. Nikulin, Pis'ma Zh. Eksp. Teor. Fiz. **15**, 30 (1972) [JETP Lett. **15**, 20 (1972)].

[8] V. P. Kuznetzov, M. A. Messerer and E. M. Omel'yanovskii, Fiz. Tekh. Poluprovodn. **18**, 446 (1984) [Sov. Phys.—Semicond. **18**, 278 (1984)].

[9] N. Puetz, G. Hillier, and A. J. SpringThorpe, J. Electron. Mater. **17**, 381 (1988).

[10] M. Benzaquen, B. Belache, C. Blaauw, and R. A. Bruce (unpublished).

[11] P. Weissfloch, M. Benzaquen, and D. Walsh, Rev. Sci. Instrum. **58**, 1749 (1987).

[12] J. S. Blakemore, *Semiconductor Statistics* (Pergamon, Oxford, 1962).

[13] C. S. Hung, Phys. Rev. **79**, 727 (1950).

[14] M. Benzaquen, K. Mazuruk, D. Walsh, C. Blauuw, and N. Puetz, J. Cryst. Growth **77**, 430 (1986).

[15] M. Benzaquen, M. Beaudoin, D. Walsh, and N. Puetz, Phys. Rev. B **38**, 7824 (1988).

[16] M. Benzaquen (unpublished).

[17] M. Benzaquen, D. Walsh, and K. Mazuruk, Solid State Commun. **61**, 803 (1987).

[18] M. Benzaquen, D. Walsh, and K. Mazuruk, Phys. Rev. B **38**, 10 933 (1988).

[19] H. Fukuyama and K. Yosida, J. Phys. Soc. Jpn. **46**, 102 (1979).

[20] B. I. Shklovskii and I. Y. Yanchev, Fiz. Tekh. Poluprovodn. **6**, 1616 (1972) [Sov. Phys.—Semicond. **6**, 1395 (1973)].

[21] M. Benzaquen and D. Walsh, J. Appl. Phys. **66**, 1206 (1989).